RKCL5529

CHARACTERIZATION OF Au-Rh AND Au-Mo BIMETALLIC NANOCLUSTERS ON TiO$_2$(110): A COMPARATIVE STUDY

János Kiss*, László Óvári, László Bugyi and András Berkó
Reaction Kinetics Research Laboratory, Chemical Research Center of the Hungarian Academy of Sciences, University of Szeged, Hungary , P.O.Box 168, H-6701 Szeged, Hungary

Abstract

Gold-rhodium and gold-molybdenum layers were prepared on a nearly stoichiometric titania and characterized by LEIS, XPS and STM. In the Au-Rh bimetallic system, Rh atoms impinged onto Au clusters pregrown on TiO$_2$(110) became covered by gold atoms. In contrast, Mo caused the disruption of gold nanoparticles.

Keywords: TiO$_2$(110), Rh, Au, Mo nanoclusters, bimetallic model catalyst

INTRODUCTION

The formation of metal nanoparticles on oxide surfaces is of great technological importance in catalysis, gas-sensorics and in different fields of materials science. TiO$_2$ has excellent properties as a support material, affecting the catalytic activity of the supported particles in an advantageous way in many cases. Both the metal-support electronic interaction, and particle restructuring can influence the reactivity [1-3]. Moreover, reducible oxides like titania can also act as an oxygen reservoir. A high dispersion of the metallic component (defined as the percentage of metal atoms in the topmost layer, with respect to the total metal content) is important to achieve high reaction rates.

The presence of a second metallic component can significantly improve the catalytic performance in several cases, assigned frequently to "ensemble" or "ligand" effects [4], as it was experienced for example in the catalytic reduction of NO on supported Rh-Ag [5], in the steam reforming of methane on supported

_____

*Corresponding author. Phone/Fax: +36-62-420-678; E-mail: jkiss@chem.u-szeged.hu

Ni-Au [6] or for the oxidation of CO on Pd-Au/TiO$_2$ [7]. Segregation or dissolution of surface atoms are key issues in bimetallic systems. Low energy ion scattering spectroscopy (LEIS), applied in the present work with He ions, is particularly useful to follow the surface composition, because it gives information only about the outermost atomic layer.

Previous studies concluded that the growth of gold and rhodium adlayers on clean TiO$_2$ followed Volmer-Weber mechanism, while XPS measurements showed that there is no chemical interaction between stoichiometric TiO$_2$ and the gold or rhodium particles [2-3,8-10]. In the case of Mo growth on TiO$_2$(110), we found that the outermost atomic layer comprises considerable amount of molybdenum and oxygen both at low and high metal coverages [11]. The reaction between TiO$_2$ and Mo is also evidenced by the shift in the Ti2p and Mo3d XPS lines, revealing that Ti is reduced, while Mo is oxidized. The oxidation state for titanium was 4, 3 and 2, in harmony with previous findings [12].

In our former study it was demonstrated by scanning tunneling microscopy (STM) and LEIS that addition of Mo to Au/TiO$_2$(110) resulted in the disruption of gold nanoparticles [11]. This led to the increase in the dispersion of gold. In the present work, we compare the behavior of Au-Mo system with that of Au-Rh system, both on TiO$_2$(110). Note that the interaction of rhodium with titania is much weaker than that of Mo corresponding to the lower activity of Rh towards oxygen.

EXPERIMENTAL

The experiments were performed in two separate ultrahigh vacuum (UHV) systems (base pressure <5 ×10^{-8} Pa). One chamber was equipped with facilities for LEIS, AES and XPS measurements. In the second one, STM and AES techniques were applied.

A Specs IQE 12/38 ion source was used for LEIS. He$^+$ ions of 800 eV kinetic energy were applied at a low ion flux equal to 0.03 μA/cm^2. The ions and electrons were analyzed by a Leybold hemispherical energy analyzer. The STM imaging was performed by electrochemically etched W-tips conditioned in situ by voltage pulses in a commercial room temperature STM system (WA-Techology).

The rutile TiO$_2$(110) single crystals were products of PI-KEM. The samples were attached to a Ta plate with a UHV compatible oxide glue (AREMCO, ceramobond 571), and could be heated with a filament placed behind the Ta plate. The sample temperature was measured by a chromel–alumel thermocouple, attached to the side of the sample with the same adhesive material. The cleanliness, composition and morphology of the surface were controlled by AES, LEIS, XPS and STM methods.

Rh, Mo and Au were deposited by an EGN4 e-beam evaporator of Oxford Applied Research at a substrate temperature of 300 K. The amount of the deposited metals is expressed in equivalent monolayers (ML), frequently used in literature, defined as the amount of metal, arranged in the close-packed (111) structure required to cover the substrate with a single atomic layer. In the STM chamber, the surface concentrations of the deposited metals were estimated from the volume of the nanoparticles separated clearly from each other.
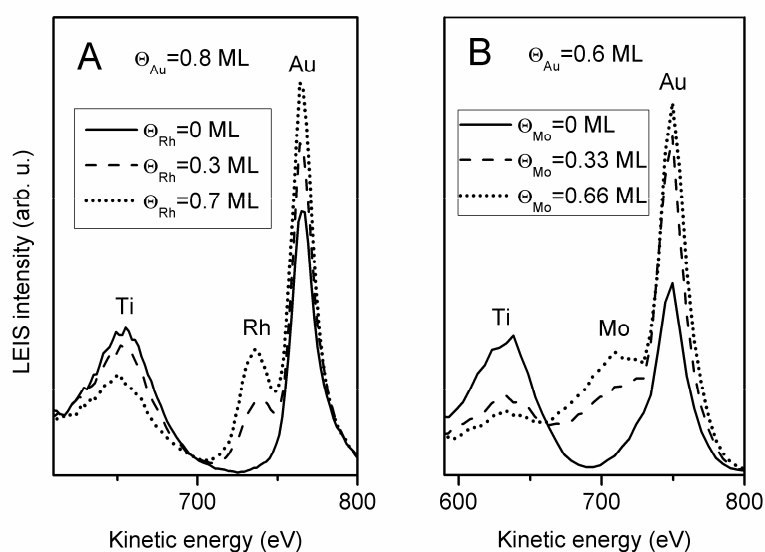

Fig. 1. (A) Ti, Rh and Au LEIS peaks as a function of Rh coverage and (B) Ti, Mo and Au LEIS signals as a function of Mo coverage, both recorded on Au-precovered titania

RESULTS AND DISCUSSION

Rh formed predominantly two dimensional (2D) clusters on titania at small coverages ($\Theta_{Rh} \leq 0.2$-0.3 ML) at room temperature according to STM and LEIS results, while 3D nanoparticles were formed at higher amounts of Rh (with a typical diameter of 1.8 nm and a height of 0.5 nm at Θ_{Rh}=0.5 ML). Gold clusters were significantly larger (diameter of 3.2 nm at Θ_{Au}=0.5 ML). Deposition of Rh on the Au/TiO$_2$(110) surface led to a decrease in the Ti and O LEIS peaks due to the shadowing effect of Rh. In contrary, a significant *increase* in the LEIS signal was detected for Au, which means that the number of Au atoms on the topmost layer of the metal clusters was enhanced (Fig. 1A). It was observed in a broad coverage range (Θ_{Au}=0.25-0.8 ML), the effect being somewhat stronger at

higher gold concentrations. Deposition of Mo on Au/TiO$_2$ resulted in rather similar changes in LEIS spectra (Fig. 1B).
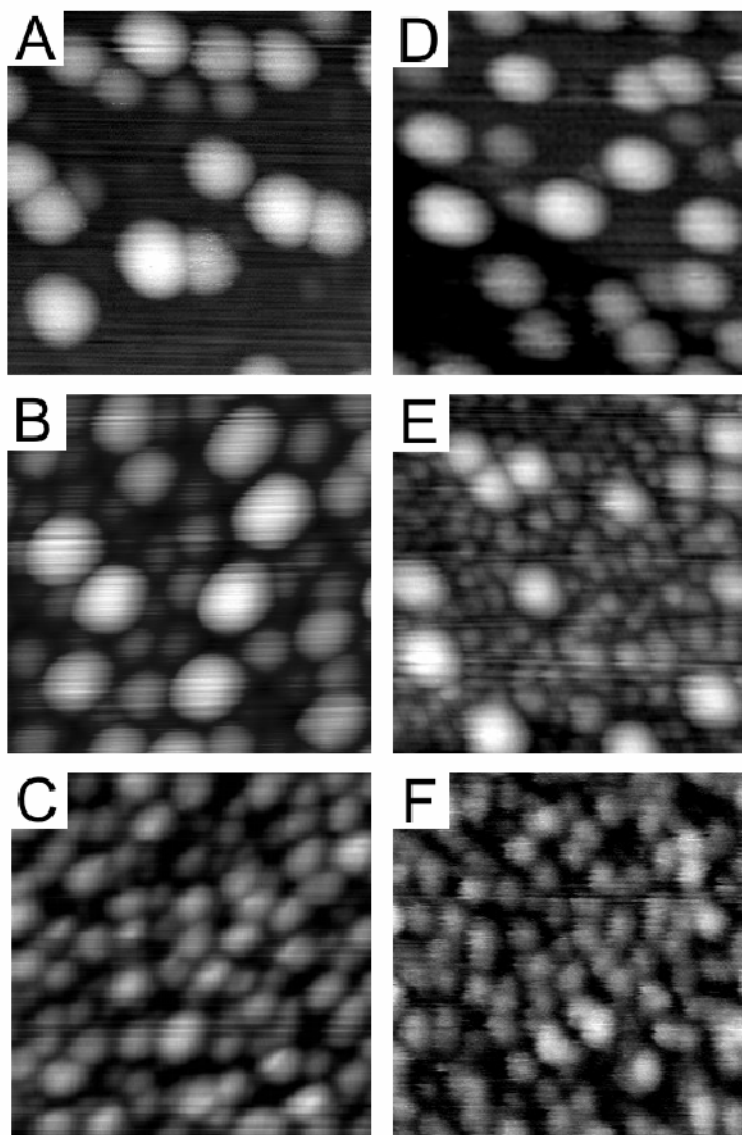
Fig. 2. STM images recorded after deposition of (A) 0.6 ML of Au; (B) 0.6 ML of Au followed by 0.6 ML Rh; (C) 0.6 ML of Rh; (D) 0.6 ML of Au; (E) 0.6 ML of Au followed by 0.3 ML Mo; (F) 0.4 ML of Mo. The size of the images: 20 x 20 nm^2

STM measurements indicated that in the case of similar coverages (Θ_{Au} and Θ_{Rh} appr. 0.5 ML) the number of Au nanoparticles did not change on the effect of the deposition of Rh. Gold clusters became larger after Rh deposition (Fig. 2 A, B, C), in contrary to what was observed for post-deposition of Mo on Au/TiO$_2$ (Fig. 2 D, E, F). The statistical evaluation, in which a raised attention was paid to tip-shape effects, exhibited an average increase of the volume of the Au particles by 60-80% on the effect of Rh post-deposition. According to the analysis of the images, a simple attachment of Rh atoms landing on Au nanoparticles during evaporation can account for an increase in the volume of the Au particles by only 20-25%. The unexpected enhancement of the average volume suggests that a fraction of rhodium atoms impinging on the free oxide surface in the vicinity of Au clusters is trapped by gold nanoparticles, while the rest of Rh formes separate rhodium clusters. Comparing LEIS and STM data, the increase in the Au LEIS peak indicates that a part of rhodium atoms evaporated on top of the gold clusters, moved to subsurface sites of gold particles. One plausible mechanism is place exchange. Both thermal and non-thermal place exchange was previously observed, when Rh was deposited on Au(111) [13,14], resulting also in the formation of subsurface Rh atoms, though the two metals are immiscible in bulk. Note that the surface energy of Au is much smaller than that of Rh. Alternatively, it seems probable that those rhodium atoms on the surface of gold clusters, which do not take part in place exchange can be covered by Au atoms diffusing on the cluster surface. Both mechanisms involve the incorporation of rhodium into the gold clusters and lead to an increase in the cluster diameter, and a concomitant enhancement in the Au LEIS signal.

In contrast, another mechanism may operate for the Mo-Au system. As the STM pictures show (Fig. 2 D,E,F), the Au particles are disrupted due to Mo deposition. The question arises why the behaviour is different for the Au-Rh and for the Au-Mo systems. Rh and Mo have similar characteristics in their relation with Au. Both metals are practically immiscible with gold [15] and have much higher surface free energies than Au (at room temperature 1.63 J/m^2 for Au, 2.83 J/m^2 for Rh and 2.88 J/m^2 for Mo [16]). A substantial difference between Rh and Mo is, however, that Mo reacts strongly with titania. As Mo reduces TiO$_2$ even at room temperature, evidenced by XPS, the reduced centers formed are responsible for the enhanced gold dispersion, since these can bind gold atoms stronger. The energy released during the reaction between Mo and surface O also may contribute to the activation of this process.

CONCLUSION

It was found by LEIS and XPS that Rh atoms impinged onto Au clusters grown beforehand on TiO$_2$(110) were covered by gold atoms through place exchange and/or surface diffusion already at room temperature. The driving force for the process is related to the surface free energies of the components. At the same time, separate Rh clusters are also formed on the gold-free oxide surface as revealed by STM measurements. In the case of Au-Mo system on titania, Mo deposition causes the disruption of gold nanoparticles. The present work clearly suggests that the parallel application of LEIS and STM techniques is very effective to explore the fine details of the supported bimetallic systems.

REFERENCES

1. C.R. Henry: *Surf. Sci. Rep.*, **31**, 231 (1998) – and references therein.
2. U. Diebold: *Surf. Sci.Rep.*, **48**, 53 (2003) – and references therein.
3. Q. Fu, T. Wagner: *Surf. Sci.Rep.*, **62**, 431 (2007) – and references therein.
4. J.A. Rodriguez: *Surf. Sci.Rep.*, **24**, 223 (1996)– and references therein.
5. O.R. Inderwildi, S.J. Jenkins, D.A. King: *Surf. Sci.*, **601**, L103 (2007).
6. J.H. Larsen, I. Chorkendorff: *Surf. Sci.Rep.*, **35**, 163 (1999) – and references therein.
7. L. Guczi: *Catal.Today*, **101**, 53 (2005) – and references therein.
8. A.M. Kiss, M. Svec, A. Berkó: *Surf. Sci.*, **600**, 3352 (2006).
9. L. Óvári, J. Kiss: *Appl. Surf. Sci.*, **252**, 8624 (2006).
10. F. Cosandey, T.E. Madey: *Surf.Rev.Lett.*, **8**, 73 (2001)– and references therein.
11. L. Bugyi, A. Berkó, L. Óvári, A.M. Kiss, J. Kiss: *Surf. Sci.*, **602**, 1650 (2008).
12. S. Pétigny, B. Domenichini, H. Mostéfa-Sba, E. Lesniewska, A. Steinbrunn, S. Bourgeois: *Appl. Surf. Sci.*, **142**, 114 (1999).
13. I. Chado, F. Scheurer, J.P. Bucher: *Phys. Rev. B*, **64**, 094410 (2001).
14. E.I. Altman, R.J. Colton: *Surf. Sci.,* **304,** L400 (1994).
15. S. Curtarolo, D. Morgan, G. Ceder: *Computer Coupling of Phase Diagrams and Thermochemistry*, **29**, 163 (2005).
16. L.Z. Mezey, J. Giber: *Jpn. J. Appl. Phys.*, **21**, 1569 (1982).